Available online at www.sciencedirect.com
ScienceDirect
Bioorganic & Medicinal Chemistry 16 (2008) 5557–5569
Bioorganic & Medicinal Chemistry

The pyridoxamine action on Amadori compounds: A reexamination of its scavenging capacity and chelating effect

Miquel Adrover, Bartolomé Vilanova,* Juan Frau, Francisco Muñoz and Josefa Donoso

Institut Universitari d'Investigació en Ciències de la Salut (IUNICS), Departament de Química, Universitat de les Illes Balears, Cra. Valldemossa km 7.5, Edifici Mateu Orfila i Rotger, E-07122 Palma de Mallorca, Spain

Received 8 February 2008; revised 26 March 2008; accepted 1 April 2008
Available online 6 April 2008

Abstract—Amadori compounds act as precursors in the formation of advanced glycation end products (AGEs) by non-enzymatic protein glycation, which are involved in ensuing protein damage. Pyridoxamine is a potent drug against protein glycation, and can act on several pathways in the glycation process. Nevertheless, the pyridoxamine inhibition action on Amadori compounds oxidation is still unclear. In this work, we have studied the Schiff base formation between pyridoxamine and various Amadori models at pH 7.4 at 37 °C in the presence of $NaCNBH_3$. We detected an adduct formation, which suggests that pyridoxamine reacts with the carbonyl group in Amadori compounds. The significance of this mechanism is tested by comparison of the obtained kinetics rate constants with that obtained for 4-(aminomethyl)-pyridine, a structural analogue of pyridoxamine without *post*-Amadori action. We also study the chelating effect of pyridoxamine on metal ions. We have determined the complexation equilibrium constants between pyridoxamine, *N*-(1-deoxy-D-fructos-1-yl)-L-tryptophan, aminoguanidine, and ascorbic acid in the presence of Zn^{2+}. The results show that the strong stability of pyridoxamine complexes is the key in its *post*-Amadori inhibition action. On the other hand results explain the lack of inhibition of aminoguanidine (a glycation inhibitor) in the *post*-Amadori reactions.

1. Introduction

Non-enzymatic glycation of long-lived proteins encompasses a complex group of reactions yielding structural and functional changes.[1,2] Such reactions are specially important in glycemic individuals and are behind diabetes-related complications including atherosclerosis,[3] renal dysfunction,[4] Alzheimer's disease,[5] and eye diseases.[6]

Protein glycation starts with the reversible condensation of carbohydrates (or dicarbonyl compounds resulting from their autoxidation) with free amino protein groups to give a Schiff base.[1e] The amino groups amenable to glycation include those on the side chains of Lys and Arg residues,[1a] and also, as recently shown, His, Trp, and Cys residues.[7] As can be seen in Scheme 1, the Schiff base formed with D-glucose as the glycating agent evolves to an *N*-(1-deoxy-D-fructos-1-yl)-L-amino acid (viz. an Amadori compound) which occurs as several forms in equilibrium.[8] Once formed, the Amadori compound can undergo dehydration and enolization, both of which are facilitated by the presence of phosphate and metal ions in the medium.[8,9] The products are two *post*-Amadori compounds (viz. an Amadori dione[10] and an Amadori ene-dione[11]) which undergo a series of complex reactions leading to the formation of advanced glycation end products (AGEs).[2] In addition, the oxidation of sugars and Schiff bases can yield radical and carbonyl species some of which are AGEs precursors as well.

In recent years, Amadori compounds have been identified as key elements in the AGEs formation in vivo[1e,12,13]; in fact, their concentrations are typically 2–3 times higher in diabetics than in healthy individuals.[14] Some authors have suggested that blocking the ketone group in an Amadori compound and their autoxidation might prevent the AGEs formation and avoid their pathological effects as a result.[13c,14] A number of inhibitors of protein glycation have been reported over the past 20 years[2d,4b,15]; none, however, has been found to directly interact with the ketone groups in Amadori compounds and prevent AGEs formation as a result.

Keywords: Amadori compound; Pyridoxamine; Kinetics; Complex formation.
* Corresponding author. Tel.: +34 971 173005; fax: +34 971 173426; e-mail: bartomeu.vilanova@uib.es

0968-0896/$ - see front matter © 2008 Elsevier Ltd. All rights reserved.
doi:10.1016/j.bmc.2008.04.002

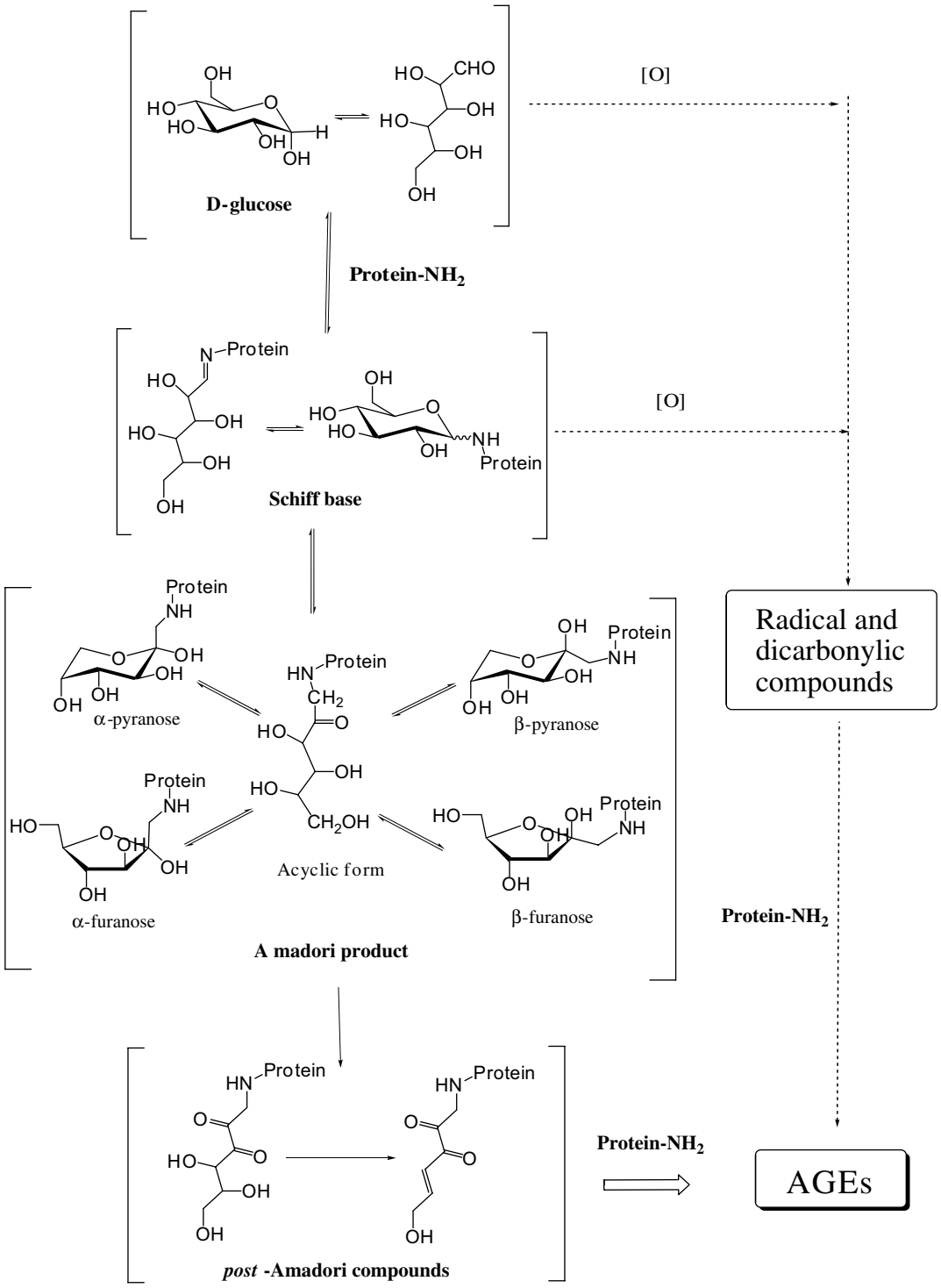

Scheme 1. Schematic representation of the non-enzymatic glycation of proteins.

Pyridoxamine is another widely studied inhibitor of AGEs formation both in vivo and in vitro.[16] The phenol and aminomethyl groups at positions 3 and 4, respectively, of its ring endow it with inhibition properties based on the following mechanisms of action: the scavenging of carbonyl species formed in the degradation of sugars and lipids[16a,c]; the inhibition of the oxidation of Amadori compounds by binding of the metal ions that catalyze the reaction[16a,g]; and scavenging of radical species by the release of the proton in the phenolate ion.[16a] Also, recent studies have shown that pyridoxamine could exhibit competitive inhibition with amino groups in proteins against glycating carbohydrates[17] and can scavenge γ-ketoaldehydes, which are involved in the development of artherosclerosis.[18]

A recent study[16b] led to the assumption that pyridoxamine is not involved in the inhibition of protein glyca-

tion by blocking the ketone group present in Amadori compounds, and its inhibition action on protein–Amadori degradation is exclusively by binding metal ions which catalyze the Amadori autoxidation.[16b] However, the fact that aminoguanidine also binds catalytic metal ions and inhibits the oxidation of ascorbic acid,[16g] but does not inhibit *post*-Amadori AGEs formation indicates that there could be other important factors involved in the efficient inhibition of *post*-Amadori reactions by pyridoxamine.

In order to clarify the mechanism of the inhibition action of pyridoxamine (**1**) on *post*-Amadori compounds, we reexamine its blocking effect on carbonyl groups present in Amadori compounds, and its chelating effect on metal ions. First, we study the Schiff bases formation between pyridoxamine (**1**) and various Amadori-models under physiological conditions of pH and temperature (Scheme 2). The studied keto compounds included acetol (**2**), which is structurally similar to the active sites in Amadori compounds; *N*-(1-deoxy-D-fructos-1-yl)-L-tryptophan (**3**), which is a model Amadori compound similar to that formed on the *N*-terminal ends of peptide chains; and 1-deoxy-1-morpholino-D-fructose (**4**), a model Amadori compound similar to that formed on Trp and His side chains (see Fig. 1). The relevance of the blocking effect by pyridoxamine is analyzed by comparing the kinetic rate constants for the Schiff bases formation with those obtained with 4-(aminomethyl)-pyridine (**5**), a structural analogue of **1**, lacking the *post*-Amadori inhibition action.[16b] The comparison of the microscopic kinetic rate constants allows us to determine the effect of the phenol group on the nucleophilic character of the aminomethyl group in **1.**

Additionally, we have determined the kinetic rate constant for pyridoxamine Schiff base formation in the presence of Zn^{2+} in order to analyze if complex formation can compete with scavenging of carbonyl species by **1**. The chelating study was completed by the analysis of the equilibrium constants for the complex formation between **1**, **3**, aminoguanidine (**6**), and ascorbic acid (**7**) with Zn^{2+} by ^{13}C NMR, in order to clarify the differences between pyridoxamine and aminoguanidine, both chelating agents which inhibit the oxidation of ascorbic acid but show different *post*-Amadori inhibition action as stated previously.

2. Results and discussion

2.1. Stability of the Amadori compounds 3 and 4

Determining kinetic constants requires an accurate knowledge of the initial reactant concentrations. This entailed checking the Amadori compounds for stability under the specific reaction conditions used (viz. pH 7.4 as adjusted with 0.5 M phosphate buffer and a temperature of 37 °C). The preliminary experiments revealed both Amadori compounds (**3** and **4**) to be unstable under such conditions; hence their kinetics parameters must be determined.

The degradation kinetics of compound **3** was monitored by HPLC. Fitting the experimental data to Eq. 1 yielded a k_{d3} $(28 \pm 1) \times 10^{-3}$ h^{-1} ($t_{1/2}$ 25 h) (see Section 4). The degradation products obtained were analysed by injecting the reaction mixture into the LC–MS system after 52 h of incubation. The chromatogram exhibited

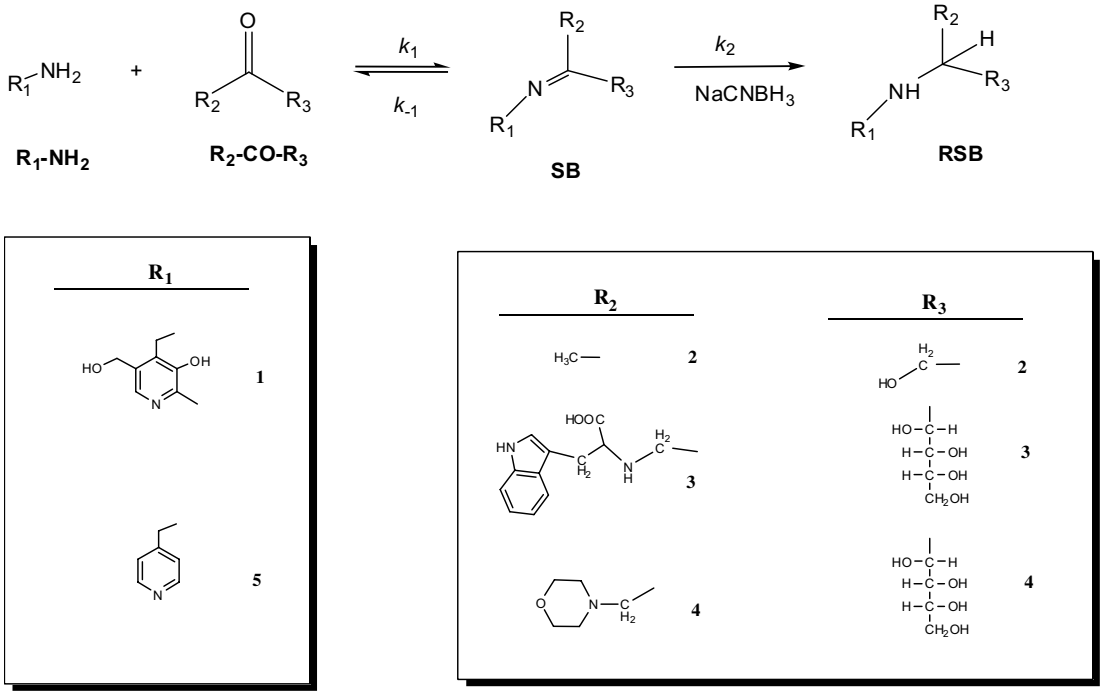

Scheme 2. Schematic representation of Schiff bases formation and subsequent reduction by $NaCNBH_3$.

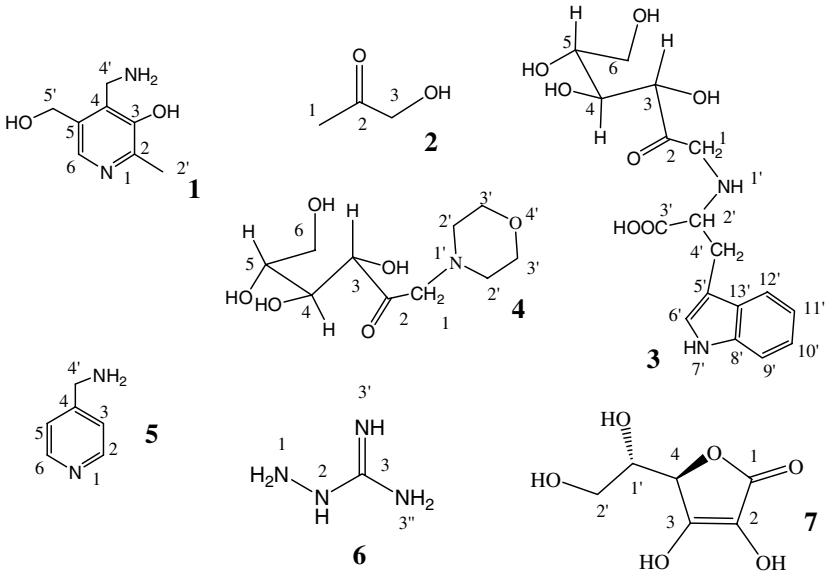

Figure 1. Structure of pyridoxamine (**1**), 4-(aminomethyl)-pyridine (**5**), aminoguanidine (**6**), ascorbic acid (**7**), and the carbonyl compounds employed in this study.

two major signals, namely: one at *m/z* 205 that was assigned to the $[M+H]^+$ peak for Trp and the other at *m/z* 219 that was assigned to the $[M+K]^+$ peak for D-glucose and D-mannose.[19]

The degradation kinetics of compound **4** was monitored by ^{1}H NMR, using area measurements of the signal at 3.35 ppm (see Section 4). Fitting the experimental data to Eq. 2 yielded k_{d4} $(7.5 \pm 1.5) \times 10^{-3}$ h^{-1} ($t_{1/2}$ 92 h). The degradation products obtained were analysed by injecting the reaction mixture into the LC–MS system after 100 h of incubation. The chromatogram exhibited a major signal at *m/z* 110 that was assigned to the $[M+Na]^+$ peak for the morpholino and another one at *m/z* 219 which was assigned to the $[M+K]^+$ peak for D-glucose and D-mannose.[19]

The degradation kinetics of the Amadori compounds **3** and **4** was also studied under the previous reaction conditions in the presence of $NaCNBH_3$. The results were similar to those obtained in the absence of the reducing agent.

2.2. Schiff base formation between pyridoxamine (1) and 4-(aminomethyl)-pyridine (5) with Amadori type compounds (2–4)

Acetol (**2**) is the simplest structural analogue of the active group in Amadori compounds. Acetol levels are increased in diabetic patients with ketosis[20] as a result of the compound being an intermediate in the transformation of acetone into methylglyoxal under the action of cytochrome P450.[21]

The reaction between **1** and **2** in the presence of $NaCNBH_3$ was followed by HPLC. The signal corresponding to **1** decreased with time as a new major signal appeared. The compound causing that signal was isolated and characterized, and assigned to compound **8** (Fig. 2, see Section 4). The fact that **8** being the end product confirms the attack of the amino group in **1** on the carbonyl group in **2** to form a Schiff base, which was subsequently selectively reduced by $NaCNBH_3$.

The evidence of former attack suggests checking this behaviour on proper Amadori compounds as **3** and **4**. Figure 3 shows the temporal variation of the chromatographic signals during the reaction between **1** and compound **3** in the presence of $NaCNBH_3$. Initially, the chromatogram exhibited the signals for compounds **1** (t_R 5 min) and **3** (t_R 52 min). Subsequently, the peak for compound **1** shrank as two new signals appeared: one at t_R 39 min corresponding to **9** (the condensation product of **1** and **3**), and the other at t_R35 min corresponding to Trp formed by the degradation of **3**. An analogous chromatographic pattern was found for the reaction of **1** and **4**, being compound **10** the final reaction product, which was characterized (see Section 4).

The presence of compounds **9** and **10** in the medium clearly proves that pyridoxamine reacts with the carbonyl groups of the Amadori compounds. When reactions between **1** and **3** (or **4**) were performed in the absence of $NaCNBH_3$, and followed over 20 h (in order to avoid degradation effects on **3** and **4**) no new chromatographic signals were observed, probably because under such conditions the equilibrium of Schiff bases formation was displaced to the reactants, so any Schiff base or derivatives formed are at undetectable levels. These results agree with other ones previously published for a similar system and similar experimental conditions.[16b]

In order to determine the importance of blocking effect in the *post*-Amadori inhibition action of **1** we also studied the reaction between 4-(aminomethyl)-pyridine (**5**) and carbonyls **2**–**4**. The reactions were followed by HPLC monitoring the decrease of **5** signals with reaction time (see Section 4).

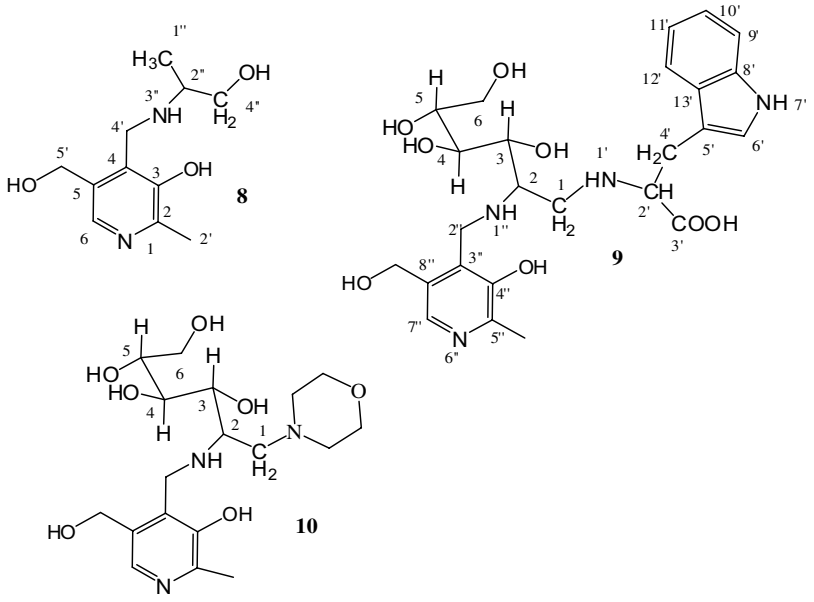

Figure 2. Structure of the identified reduced Schiff bases.

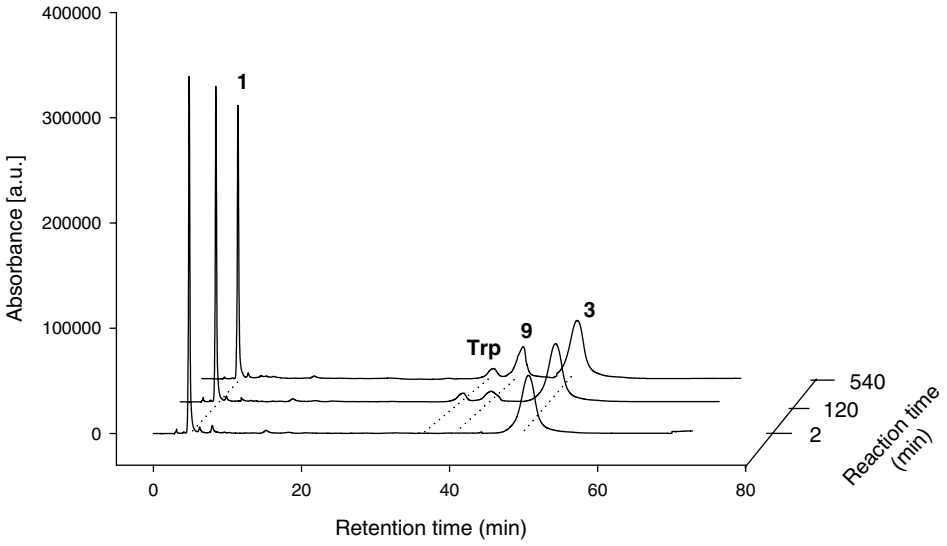

Figure 3. Time-dependent HPLC chromatograms for the reaction between 0.01 M pyridoxamine (**1**) and 0.2 M *N*-(1-deoxy-D-fructos-1-yl)-L-tryptophan (**3**) in a phosphate-buffered medium at pH 7.4 at 37 °C in the presence of $NaCNBH_3$. UV/vis detection at 305 nm.

Figure 4 shows that the temporal variation of **1** and **5** concentrations in each of the previous reactions follows a *pseudo* first-order kinetics (Eq. 20). The k_{obs} values obtained by the treatment of these experimental data are depicted in Table 1. The table also shows values for k_1, the microscopic kinetic rate constant for Schiff base formation (calculated from Eq. 18 for **1** and from Eq. 23 for **5**). In these calculations, the apparent tautomeric equilibrium constant between the reactive tautomer of pyridoxamine (**1a**) and the other tautomers present in the medium at the working pH, K_3 in Scheme 3, was taken to be 0.036.[17a] The dissociation constant for the aminomethyl group in **5** (K_6) was determined at 25 °C by other authors.[22] This value and the knowledge of enthalpies of ionization of aliphatic amines ($\Delta H^0 \approx 13$ kcal/mol[23]) allowed us to estimate K_6 value at 37 °C such as 1.58×10^{-9} M by using Van't Hoff equation. Furthermore, based on the previous results of Glushonok et al.,[24] we adopted a value of 49 for the equilibrium constant between the carbonyl and hydrated tautomers of acetol, K_4. Taking into account that only 4.7% of compound **3** was in its carbonyl form,[25] and the structural similarities between **3** and **4**, we used a value of 5.2×10^{-2} for K_5, the equilibrium constant between the linear anomer and the different cyclic anomers.

The microscopic kinetic rate constant (k_1) values for **1** are two times smaller than those for **5**. This result agrees with the different electronic charges on the nitrogen

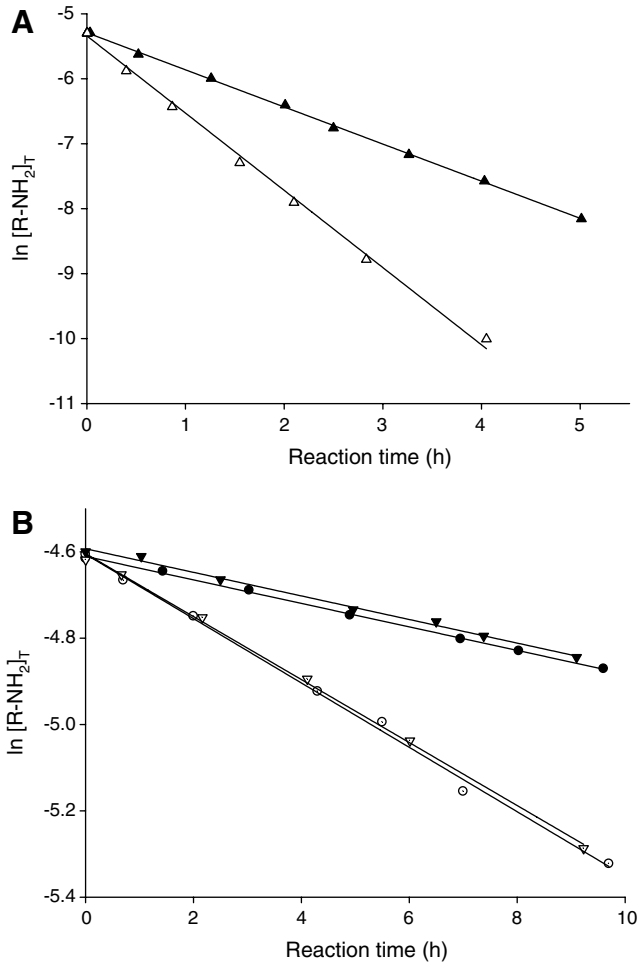

Figure 4. (A) First-order loss of pyridoxamine (▲) and 4-(aminomethyl)-pyridine (△) at an initial concentration of 0.005 M in the presence of 0.2 M of acetol (**2**), at pH 7.4 and 37 °C. (B) First-order loss of pyridoxamine (*black symbols*) at an initial concentration of 0.01 M in its reaction with 0.2 M of compound **3** (▼) and with 0.2 M of compound **4** (●). First-order loss of 4-(aminomethyl)-pyridine (*white symbols*) at an initial concentration of 0.01 M in its reaction with 0.2 M of compound **3** (▽) and with 0.2 M of compound **4** (○). All the reaction mixtures were incubated in phosphate-buffered aqueous solutions at pH 7.4 at 37 °C in the presence of $NaCNBH_3$. The slopes of the curves were used to calculate the corresponding *pseudo*-first order rate constants (k_{obs}) by using Eq. 20.

atom present in the aminomethyl group in **1a** (the reactive tautomer) and the unprotonated species of **5**. The charge on N of **5** is ca. 0.20*e* greater than that obtained for **1a**, due to the intramolecular hydrogen bond formed between N atom and the proton of phenolate in **1a**, which is absent in **5** (see Section 4.10). The obtained k_{obs} values for **5** are ca. two times higher than those for **1**, and are also due to their different nucleophilic characters, instead both presents similar proportion of unprotonated species at neutral pH (≈3.5%).

The microscopic kinetic rate constants (k_1) for **1** and Amadori compounds are 1000 times smaller than those determined for **1** with aldehydic compounds,[17] and agrees with the different electrophilic characters between ketone and aldehydic groups. The k_{obs} values obtained for **1** with **2** are greater than those obtained with the Amadori compounds **3** and **4**, as a result of the increased proportion of the carbonyl tautomer.

Our results demonstrate that pyridoxamine reacts with the Amadori compound yielding a Schiff base. The addition of reducing agent into the reaction mixture let us to detect the adduct formation and determine k_{obs} and k_1 values. The comparison of the kinetic results between **1** and **5** (an analogue of **1** without *post*-Amadori inhibition action)[16b] reveals that blocking carbonyl group in Amadori compound by **1** is not the main step in *post*-Amadori inhibition action of **1**.

2.3. Chelating effect: complex formation between 1, 3, 6, and 7 with Zn^{2+}

It has been widely described that pyridoxamine can form complexes with divalent cations. In order to check the significance of that reaction on the availability of pyridoxamine to scavenge carbonyl groups, we study the reaction between **1** and **2** in the presence of Zn^{2+}. Although Cu^{2+} catalyses the oxidation process on Amadori compounds,[16b] we use Zn^{2+} in this study in order to avoid the formation of copper hydroxide that precipitates at neutral pH. Complex formation between **1** and Zn^{2+} or Cu^{2+} involves the six coordinate ions which lie at the center of symmetry and are chelated to two **1** ligands through the amino and phenolate groups[26,27] and stabilized by two water molecules. According to complex geometry and complexes stabilities (Irving-Williams series[28]) the chelating results obtained for Zn^{2+} should agreed with those obtained for Cu^{2+}.

The reaction between **1** and **2** in the presence of $NaCNBH_3$ and Zn^{2+} was analyzed by HPLC monitoring with the decrease of **1** signal with reaction time. The reaction product **(8)** was the same as that produced without metal addition. For a metal concentration up to 2 mM, the k_{obs} values (0.58–0.45 $M^{-1}\,h^{-1}$) are similar to those obtained without metal addition. This result

Table 1. Kinetic constants for the reactions of pyridoxamine (**1**) and 4-(aminomethyl)-pyridine (**5**) with Amadori type compounds (**2**–**4**)

Reactions at pH 7.4 at 37 °C in presence of $NaCNBH_3$	k_{obs} (h^{-1})	k_1 ($M^{-1}\,h^{-1}$)
Pyridoxamine (**1**) + Acetol (**2**)	$(58 \pm 1) \times 10^{-2}$	85 ± 15
Pyridoxamine (**1**) + Amadori compound **3**	$(27 \pm 0.6) \times 10^{-3}$	83 ± 16
Pyridoxamine (**1**) + Amadori compound **4**	$(27 \pm 0.3) \times 10^{-3}$	83 ± 14
4-(Aminomethyl)-pyridine (**5**) + Acetol (**2**)	$(12 \pm 0.3) \times 10^{-1}$	157 ± 10
4-(Aminomethyl)-pyridine (**5**) + Amadori compound **3**	$(72 \pm 1.6) \times 10^{-3}$	194 ± 40
4-(Aminomethyl)-pyridine (**5**) + Amadori compound **4**	$(71 \pm 7.6) \times 10^{-3}$	190 ± 30

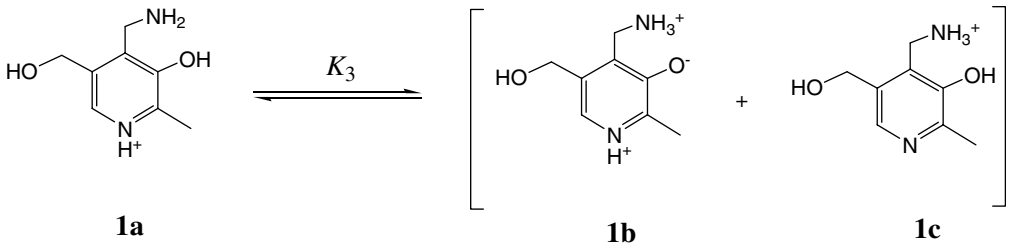

1a **1b** **1c**

Scheme 3. Tautomeric forms of pyridoxamine at pH 7.4.

shows that complex formation does not modify the capacity of **1** to react with carbonyl groups when they are in a ratio similar to that observed in vivo models under **1** treatment.[29,30]

The complexation reactions take a crucial role in the pyridoxamine inhibition of radical and *post*-Amadori AGEs formation.[16a] In contrast, there are other inhibitors of glycation processes with chelating capacity that do not inhibit *post*-Amadori reactions. One of them is aminoguanidine (**6**) that can form complexes with divalent metal ions,[31] similarly to **1**, and inhibit the oxidation of ascorbic acid (**7**),[16g] but is completely inactive as the inhibitor of *post*-Amadori oxidation.[16f]

In order to analyze the different inhibition actions between **1** and **6**, we determine the equilibrium constants for the complex formation of **1**, **3**, **6**, and **7** with Zn^{2+} by ^{13}C NMR spectroscopy. Figure 5 represents the free ligand concentration versus total Zn^{2+} concentration in citrate buffer 0.5 M at pH 7.0. Results show that **1** exhibits the highest chelating effect followed by compound **3**. In contrast, **6** shows a minor chelating effect in comparison to **1** and **3**. Under experimental conditions, it has not been possible to detect the complex formation between **7** and Zn^{2+}. Values of $K_{[Zn(1)_2-(H_2O)_2]}$ $(2.5 \pm 1.3) \times 10^3\ M^{-2}$; $K_{[Zn(3)_2-(H_2O)_2]}(4.6 \pm 0.43) \times 10^2\ M^{-2}$; $K_{[Zn(6)_2-(H_2O)_2]}$ $(1.11 \pm 0.16) \times 10^2\ M^{-2}$ were obtained by fitting the experimental results to Eq. 4 . The

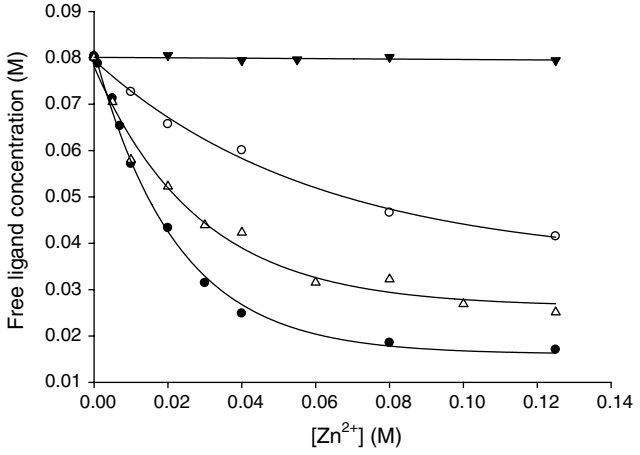

Figure 5. Plot of free ligand concentration versus total Zn^{2+} concentration in 0.5 M citrate buffer at pH 7.0 at room temperature. The initial ligand concentration was 0.08 M for all the compounds. Compounds **1** (●), **3** (△), **6** (○), and **7** (▼) were used as ligands.

highest stability of $[Zn(\mathbf{1})_2–(H_2O)_2]$ with respect to **3**, **6**, and **7** complexes causes the metal ions to bind preferentially to **1** instead of Amadori compounds, inhibiting Amadori autoxidation as a result. This result agrees with experimental data that demonstrates that **1** can inhibit the catalysis of metal ions on *post*-Amadori reactions.[16b]

Khalifa et al.[16f] have shown that although aminoguanidine is a chelating agent, it does not present inhibition action in *post*-Amadori reactions. The minor chelating effect of **6** in comparison to the Amadori compound explains this lack in the inhibition action. Since the equilibrium constant is lower than that for Amadori compounds and higher than that for **7**, compound **6** can only inhibit the metal catalyzed oxidation of **7**, as corroborated by experimental data.[16g]

3. Conclusions

The results obtained in this work clearly show that pyridoxamine (**1**) reacts with the carbonyl group in model Amadori compounds in the presence of $NaCNBH_3$. Nevertheless, the similar reactivity of **1** and **5** (compound without *post*-Amadori inhibition action) with the Amadori compounds reveals that the blocking effect of **1** is not significant in the inhibition of *post*-Amadori AGEs formation. The strong pyridoxamine inhibition of *post*-Amadori reactions is due to the metal chelation. Results confirm that pyridoxamine efficiently sequesters metal ions away from Amadori-complexes. In contrast, aminoguanidine, due to its lower metal chelation effect, cannot inhibit the *post*-Amadori reactions. Finally, both **1** and **6** can inhibit the oxidation of **7**.

Our results suggest that a good *post*-Amadori inhibitor compound should form a stable metal ion complex with an equilibrium constant higher than that for the Amadori compounds, which is supported by the fact that strong chelators such as EDTA or DETAPAC can also inhibit protein modification.[32]

4. Experimental

4.1. Materials

Pyridoxamine dihydrochloride, 1-deoxy-1-morpholino-D-fructose, D_2O (99.9% D), 4-(aminomethyl)-pyridine, aminoguanidine hydrochloride, ascorbic acid, and D-glu-

cose were purchased from Sigma–Aldrich; acetol was obtained from Fluka; and sodium cyanoborohydride, L-tryptophan, potassium dihydrogen phosphate, sodium citrate, methanol, $ZnCl_2$, and acetone were supplied by Acros Organics. All were used as received. The buffering material was reagent-grade and Milli-Q water used throughout.

4.2. High performance liquid chromatography (HPLC)

HPLC analyses were performed on a *Shimadzu-LC 10AT* chromatograph equipped with a *Rheodyne 7725i* universal injector and a *Shimadzu SPD-M20A* UV/vis photodiode array detector. The column was a *Tracer Excel 120 ODBS* model (25×0.46 cm, 5 μm). A MeCN/water gradient was used to separate the target compounds in the study of the degradation of compound **3**, and one of MeCN/water–50 mM potassium phosphate (pH 6.0) was employed to separate those in the other reaction mixtures.

4.3. NMR spectroscopy

NMR spectra were recorded on a *Bruker AMX-300* spectrometer, using sample tubes of 5 mm in diameter and 3-(trimethylsilyl)-1-propanesulphonic acid (DSS) as an internal standard. All the chemical shifts for ^1H (δ_H) and ^{13}C (δ_C) are given in parts per million. The solutions used for products characterization were prepared in D_2O, and were stabilized at p*D* 7.4 (p*D* = −log $[D^+]$) with 0.5 M phosphate buffer. The reaction mixtures for the study of complex formation between **1**, **3**, **6**, and **7** with Zn^{2+} were prepared in citrate buffer 0.5 M at pH 7.0, using a mixture of H_2O/D_2O (80:20) in order to avoid the zinc phosphate precipitation. ^{13}C multiplicities were calculated by using the distortionless enhancement bipolarization transfer method (DEPT-135),[33] and ^1H–^1H and ^{13}C–^1H correlations were determined from two-dimensional heteronuclear measurements (H,H-COSY; H,C-HMQC).[34]

4.4. UV/vis spectra

The absorption spectra for compounds **1** and **3** were recorded at room temperature on a *Shimadzu UV-2401 double-beam recording spectrophotometer* furnished with quartz cells of 1 cm path length.

4.5. LC–MS analysis

Mass analyses were performed on an *Agilent 1110 Series LC–MS instrument*. The mass spectra for compound **3**, **8**, and **9** were obtained by columnless flow injection analysis (FIA). The mass spectrum for compound **10** was obtained by injecting the reaction mixture through a *Tracer Excel 120 ODBS* column (25×0.46 cm, 5 μm). Mass spectral detection of the compounds was accomplished by using an electrospray ionization interface and a quadrupole mass analyser. The mobile phase was 5 mM ammonium acetate at pH 6.0—NH_4OAc initiates the ionization for MS detection—and circulated at a flow-rate of 0.3 ml/min. The mobile phase was nebulized into an electrospray mass analyser by using gaseous nitrogen at 350 °C at a flow-rate of 13 ml/min. The detector was used to count positive ions over the *m*/*z* range 100–800 in the scan mode. A nebulization pressure of 415.6 kPa, a fragmentor voltage of 80 V, and a capillary voltage of 3000 V were used.

4.6. Synthesis of *N*-(1-deoxy-D-fructos-1-yl)-L-tryptophan trihydrate (3)

Compound **3** was prepared by using a modified version of the method of Beksan et al.[35] for *N*-(1-deoxy-D-fructos-1-yl)-L-glutamic acid. A solution of potassium hydroxide (0.58 g) in methanol (12 ml) was added to L-tryptophan (3 g) and the mixture stirred until the amino acid was completely dissolved. A solution of anhydrous D-glucose (1.5 g) in methanol (15 ml) was then added and the resulting suspension refluxed at 70 °C with stirring for 2 h. After cooling to room temperature, the reaction volume was reduced to 10 ml under vacuum, excess amino acid removed by filtration, and the filtrate cooled to 0 °C. Addition of acetone caused a precipitate in the form of an amorphous yellow powder to be formed that was purified by vacuum filtration and re-dissolution in methanol. The precipitate was refluxed in a mixture of methanol (10 ml) and acetic acid (0.2 ml) at 70 °C for 30 min. Following cooling, the addition of acetone gave a new precipitate that was filtered and purified by vacuum filtration, re-dissolution in methanol, and re-precipitation with acetone. The solid thus obtained was a pale brown amorphous powder that was dissolved in water and lyophilized to obtain *N*-(1-deoxy-D-fructos-1-yl)-L-tryptophan (29% yield). LC/MS: *m*/*z* 405.09 $[M+K]^+$ (100), 367.14 $[M+H]^+$ (79), 389.13 $[M+Na]^+$ (68), 349.14 $[M-H_2O]^+$ (35). ^1H NMR, H,H-COSY, arbitrary numbering on carbon atoms refers to major anomeric form (β-pyranose)[36] of **3** in Figure 2: δ 7.55 (d, 1H, $^3J_{H11'-H12'} = 8.0$ Hz, H-C(12′)); 7.37 (d, 1H, $^3J_{H9'-H10'} = 8.0$ Hz, H-C(9′)); 7.17 (s, 1H, H-C(6′)); 7.13 (dd, 1H, $^3J_{H10'-H11'} = 7.1$ Hz, H-C(10′)); 7.04 (dd, 1H, H-C(11′)); 3.89 (dd, 1H, $^3J_{H2'-H4'A} = 5.6$ Hz, $^3J_{H2'-H4'B} = 7.0$ Hz, H-C(2′)); 3.77 (m, 1H, $^3J_{H4-H5} = 3.0$ Hz, $^3J_{H5-H6A}$=1.0 Hz, $^3J_{H5-H6B} = 2.2$ Hz, H-C(5)); 3.63 (dd, 1H, $^3J_{H3-H4} = 9.3$ Hz, H-C(4)); 3.49 (d, 1H, H-C(3)); 3.44 and 3.77 (dd, 2H, $^2J_{H6A-H6B} = 12.3$ Hz, H-C(6)); 3.29 and 3.33 (dd, 2H, $^2J_{H4'A-H4'B} = 15.1$ Hz, H-C(4′)); 3.03, 3.19 (d, 2H, $^2J_{H1A-H1B}$=12.2 Hz, H-C(1)). ^{13}C NMR, HMQC, DEPT-135: δ 175.6 C(3′); 138.9 C(8′); 129.2 C(13′); 127.6 C(6′); 124.7 C(11′); 122.1 C(10′); 121.1 C(12′); 114.5 C(9′); 109.6 C(5′); 97.6 C(2); 72.9 C(3); 71.8 C(4); 71.3 C(5); 66.3 C(6); 65.7 C(2′); 55.5 C(1); 28.3 C(4′). The spectral data were consistent with others previously determined for compound **3** by Röper et al.[36] UV λ_{max} 279. Anal. Calcd. for $C_{17}H_{22}N_2O_7 \cdot 3H_2O$ (420.16): C, 48.57; H, 6.71; N, 6.66; O, 38.06. Found: C, 49.85; H, 6.29; N, 6.63; O, 37.37.

4.7. Reaction mixtures for kinetic and thermodynamic studies

4.7.1. Kinetic study of the stability of compounds 3 and 4. A solution containing a 1 mM of compound **3** in 0.5 M phosphate buffer at pH 7.4 at 37 °C was used to monitor

its degradation kinetics by using HPLC to measure the area of its chromatographic peak at 280 nm. The experimental data were fitted to Eq. 1 in order to calculate the degradation constant of **3** (k_{d3})

$$\ln\frac{[3]}{[3]_0} = -k_{d3}t \quad (1)$$

The degradation kinetics of **4** was studied by ^{1}H NMR spectroscopy, using a 5 mM solution of the compound in 0.5 M phosphate buffer at p*D* 7.4 at 37 °C. The kinetics was monitored by measuring the area of a triplet signal at 3.35 ppm corresponding to the protons on C(2′) in the resulting morpholino. The experimental data were fitted to Eq. 2 by using the software SigmaPlot v. 9.0[37] in order to calculate the degradation constant for the compound (k_{d4})

$$[4] = [4]_0\left(1 - e^{(-k_{d4}t)}\right) \quad (2)$$

4.7.2. Kinetic study of the interaction between pyridoxamine (1) with compounds 2–4. Phosphate buffer (0.5 M) at pH 7.4 was used to prepare the following reaction mixtures: (a) 5 mM **1** + 0.1 M $NaCNBH_3$ + 0.2 M **2**; and (b) 10 mM **1** + 0.1 M $NaCNBH_3$ + 0.2 M compound **3** or **4**. To analyze the effect of metal binding on the kinetic rate constant for the Schiff base formation from **1**, the following reactions were prepared in 0.5 M citrate buffer at pH 7.4: (c) 5 mM **1** + 0.1 M $NaCNBH_3$ + 0.2 M **2** + 0.1 mM $ZnCl_2$; (d) 5 mM **1** + 0.1 M $NaCNBH_3$ + 0.2 M **2** + 0.5 mM $ZnCl_2$; (e) 5 mM **1** + 0.1 M $NaCNBH_3$ + 0.2 M **2** + 1 mM $ZnCl_2$; (f) 5 mM **1** + 0.1 M $NaCNBH_3$ + 0.2 M compound **2** + 2 mM $ZnCl_2$. The addition of $NaCNBH_3$ can selectively reduce imino groups while leaving carbonyl groups intact at physiological pH,[38] and it has previously been used to determine the kinetic formation constants for various Schiff bases.[39] Although it has been reported that *N*-cyanomethyl products can be formed in the reductive methylation of proteins with formaldehyde and $NaCNBH_3$,[40] in this work, we have not detected the formation of any *N*-cyanomethyl product. These solutions were thermostated at 37 °C throughout. The reaction kinetics was monitored by making HPLC measurements of the chromatographic peak at 321 nm for compounds **2** and **4**, and that at 305 nm for **3**, at different times.

4.7.3. Kinetic study of the interaction between 4-(aminomethyl)-pyridine (5) with compounds 2 – 4. Phosphate buffer at a 0.5 M concentration and pH 7.4 was used to prepare the following reaction mixtures: (a) 5 mM **5** + 0.1 M $NaCNBH_3$ + 0.2 M **2** and (b) 10 mM **5** + 0.1 M $NaCNBH_3$ + 0.2 M compound **3** or **4**. The three solutions were thermostated at 37 °C throughout. The reaction kinetics was monitored by making HPLC measurements of the chromatographic peak at 257 nm at different times.

4.7.4. Thermodynamic study of the complex formation between 1, 3, 6, and 7 with Zn^{2+}. Solutions 0.08 M of **1**, **3**, **6**, and **7** containing each one escalating concentrations from 0.001 to 0.125 M of $ZnCl_2$ were prepared in 0.5 M citrate buffer at pH 7.0 (20% in D_2O). The equilibrium constants were determined by ^{13}C NMR measurements. ^{13}C chemical shifts (ppm) for **1**, **3**, and **6** as free ligands and in 1:2 adducts with Zn^{2+} are depicted in Table 2. The ^{13}C NMR signal of citrate appeared at 184.5 ppm is not affected by increasing Zn^{2+} concentration, and was taken as a reference. For pyridoxamine the study was followed by analyzing the decrease of height peak corresponding to C(2) (135.2 ppm). For **3** the equilibrium was analyzed by taking into account the decrease of height of C(5′) signal (109.6 ppm) since metal ion binding to N(1′) and carboxylic group in C(3′) affect to C(5′) signal, as was described by other authors.[41] Same results were obtained by analyzing the decrease of intensity signals corresponding to C(2′) or C(4′). For compound **6**, the increase in the signal at 161.6 ppm corresponding to C(3) is due to the change in its relaxation time as has been described in complex formation.[42] For compound **7** C(2) and C(3) signals were taken to determine its complex formation since its dienol group is the most probable centre in chelating process.[43] The equilibrium to complex formation is described by the following equation:

$$Zn^{2+} + 2L \underset{}{\overset{K_{[Zn(L)_2-(H_2O)_2]}}{\rightleftharpoons}} [Zn(L)_2-(H_2O)_2] \quad (3)$$

Table 2. ^{13}C chemical shifts (ppm) for **1**, **3**, **6**, and **7** as free ligands and in 2:1 adducts with Zn^{2+}

Pyridoxamine (**1**)[a]	*Free ligand:* C(2′):17.8; C(4′): 38.9; C(5′): 61.7; C(6): 126.1; C(2): 135.2; C(4): 138.5; C(5): 147.5; C(3): 165.5 *Complex:* C(2′):18.0; C(4′): 40.1; C(5′): 61.7; C(6): 126.4; C(2): –; C(4): 138.3; C(5): 147.6; C(3): 168.0
Amadori compound **3**[a]	*Free ligand:* C(4′): 28.3; C(1): 55.5; C(2′): 65.7; C(6): 66.3; C(5): 71.3; C(4): 71.8; C(3): 72.9; C(2): 97.6; C(5′): 109.6; C(9′): 114.5; C(12): 121.1; C(10′): 122.1; C(11′): 124.7; C(6′): 127.6; C(13′): 129.2; C(8′): 138.9; C(3′): 175.6 *Complex:* C(4′): 29.2; C(1): 56.2; C(2′): 66.0; C(6): 66.2; C(5): 71.5; C(4): 72.0; C(3): 72.9; C(2): 98.8; C(5′): 110.9; C(9′): 114.6; C(12): 121.2; C(10′): 122.0; C(11′): 124.6; C(6′): 127.7; C(13′): 129.3; C(8′): 139.0; C(3′): –
Aminoguanidine (**6**)	*Free ligand:* C(3): 161.6 *Complex:* C(3): 161.5
Ascorbic acid (**7**)[b]	*Free ligand:* C(2′): 65.3; C(1′): 72.2; C(4): 81.0; C(2): 115.7; C(3): 178.15; C(1): 180.0

[a] Some signals (C(2) in **1** and C(3′) in **3**) present in the free ligand disappeared in the complex compound. This effect has been previously describe in metal complex studies by ^{13}C NMR.[41,44]

[b] We have not detected any change in the ^{13}C NMR signals as a result of increase of Zn^{2+} concentration.

where L represents 1, 3, 6, and 7. The equilibrium constant is given by the following equation:

$$K_{[Zn(L)_2-(H_2O)_2]} = \frac{[Zn(L)_2-(H_2O)_2]}{[Zn^{2+}][L]^2} \quad (4)$$

4.8. Products identification

4.8.1. Reduced Schiff base formed between pyridoxamine (1) and acetol (2): 4-((1-hydroxypropan-2-ylamino)methyl)-5-(hydroxymethyl)-2-methylpyridin-3-ol (8). After a reaction time of 10 h, an aliquot (20 ml) of the reaction mixture between **1** and **2** described above was purified by HPLC. The new peak that appeared at t_R 33.9 min was isolated, freeze–dried, and characterized by NMR in 0.5 M phosphate buffer at p*D* 7.4. ^{1}H NMR: δ 7.66 (s, 1H, H-C(6)); 4.82(s, 2H, C(4′)); 4.71 (s, 2H, C(5′)); 4.41 (m, 2H, $^2J_{H4''A-H4''B} = 12.6$ Hz, $^3J_{H4''A-H2''}$ 3.7 Hz, H-C(4″A)); 3.65 (m, 1H, $^3J_{H2''-H1''} = 6.7$ Hz, $^3J_{H2''-H4B''} = 4.3$ Hz, H-C(2″)); 3.87 (m, 2H, H-C(4″B)); 2.49 (s, 3H, C(2′)); 1.35 (d, 3H, H-C(1″)). ^{13}C NMR, DEPT-135: δ 165.2 C(3); 146.7 C(4); 138.3 C(5); 133.7 C(2); 125.4 C(6); 69.4 C(4″); 61.2 C(5′); 57.2 C(2″); 44.0 C(4′); 17.7 C(2′); 14.8 C(1″). The molecular weight of the isolated compound was determined by LC–MS system. The obtained mass spectrum shows a major signal *m*/*z* 227 according to the $[M+H]^+$ peak for **8**. The NMR and mass spectra data confirm compound **8** such as the major product formed in the reaction between pyridoxamine and acetol under reductive conditions.

4.8.2. Reduced Schiff base of pyridoxamine with compound 3: compound 9. After a reaction time of 20 h, an aliquot (10 ml) of the reaction mixture between **1** (0.1 M) and **3** (0.04 M) was purified by HPLC. The peak that appeared at t_R 39 min (Fig. 3) was isolated, freeze–dried, and characterized by NMR in 0.5 M phosphate buffer at p*D* 7.4. ^{1}H NMR: δ 7.65 (s, 1H, H-C(7″)); 7.55 (d, 1H, $^3J_{H12'-H11'} = 7.9$ Hz, H-C(12′)); 7.36 (d, 1H, $^3J_{H9'-H10'} = 7.9$ Hz, H-C(9′)); 7.17 (s, 1H, H-C(6′)); 7.13 (dd, 1H, $^3J_{H10'-H11'} = 7.4$ Hz, H-C(10′)); 7.04 (dd, 1H, H-C(11′)); 4.88 (s, 2H, C(2″)); 4.73 (s, 2H, CH_2-C(8″)); 3.90 (dd, 1H, $^3J_{H2'-H4'A} = 5.4$ Hz, $^3J_{H2'-H4'B} = 7.2$ Hz, H-C(2′)); 3.77 (m, 1H, $^3J_{H4-H5} = 3.2$ Hz, $^3J_{H5-H6A} = 1.3$ Hz, $^3J_{H5-H6B} = 2.2$ Hz, H-C(5)); 3.62 (dd, 1H, $^3J_{H4-H3} = 8.2$ Hz, H-C(4)); 3.57 (m, 1H, $^3J_{H2-H1} = 5.3$ Hz, $^3J_{H2-H3} = 4.4$ Hz, H-C(2)); 3.50 (m, 1H, H-C(3)); 3.40 and 3.72 (dd, 2H, $^2J_{H6A-H6B}$=12.2 Hz, H-C(6)); 3.32 and 3.28 (dd, 2H, $^2J_{H4'A-H4'B} = 15.1$ Hz, H-C(4′)); 2.79, 2.53 (m, 2H, $^2J_{H1A-H1B} = 12.0$ Hz, H-C(1)); 2.48 (s, 3H, CH_3-C(5″)). ^{13}C NMR, DEPT-135: δ 176.2 C(3′); 165.0 C(4″); 146.9 C(3″); 138.9 C(8′); 138.5 C(8″); 135.1 C(5″); 129.2 C(13′); 127.6 C(6′); 126.0 C(7″); 124.74 C(11′); 122.0 C(10′); 121.1 C(12′); 114.2 C(9′); 109.0 C(5′); 75.0 C(4); 73.9 C(3); 73.4 C(5); 66.3 C(6); 65.5 C(2′); 61.7 CH_2-C(8″); 58.7 C(2); 49.5 C(1); 44.4 C(2″); 28.3 C(4′); 17.3 CH_3-C(5″). The molecular weight of the isolated compound was determined by LC–MS system. The obtained mass spectrum shows a major signal *m*/*z* 519 according to the $[M+H]^+$ peak for **9**. The NMR and mass spectra data confirm the condensation of compounds **1** and **3**, and the subsequent reduction of the formed Schiff base (**9**). The UV/vis spectrum for compound **9** exhibits the two typical bands for compound **1** at the working pH (256 and 325 nm) in addition to the typical band for **3** (279 nm); this provides additional experimental evidence for a condensation reaction between **1** and the Amadori compound **3**.

4.8.3. Reduced Schiff base of pyridoxamine with compound 4: compound 10. A reaction mixture containing a 0.15 M concentration of compound **4**, 0.2 M **1** and 0.2 M $NaCNBH_3$ in 0.5 M phosphate buffer at p*D* 7.4 at 37 °C was subjected to ^{13}C NMR and DEPT-135 analysis. The initial spectra exhibited the expected signals for **1**[17a] and compound **4**.[45†] A new analysis of the reaction mixture after 4 h of incubation revealed the disappearance of the ^{13}C NMR signals for C(2) in compound **4** and the appearance of a new one at 55.8 ppm corresponding to a tertiary compound that was assigned to C(2) in compound **10**. This result confirms the condensation of compounds **1** and **5** to form the reduced Schiff base **10** (see Fig. 4). The molecular weight of **10** was determined by injecting the reaction mixture into the LC–MS system. The result was three chromatographic signals at *m*/*z* 169, 250, and 402 corresponding to the $[M+H]^+$ peaks for **1**, compound **4**, and compound **10**, respectively.

4.9. Determination of Schiff base formation rate constant

Scheme 2 shows the kinetic mechanism for the formation of the Schiff base and subsequent reduction by sodium cyanoborohydride. The rates of disappearance of compounds **1** and **5** from the reaction medium conformed to the following law:

$$\frac{-d[R_1\text{-}NH_2]}{dt} = k_1[R_2\text{-CO-}R_3][R_1\text{-}NH_2] - k_{-1}[SB] \quad (5)$$

Application of the steady-state approximation to the Schiff base yields

$$\frac{-d[SB]}{dt} = k_1[R_2\text{-CO-}R_3][R_1\text{-}NH_2] - k_{-1}[SB] - k_2[SB] = 0 \quad (6)$$

Therefore,

$$[SB] = \frac{k_1[R_2\text{-CO-}R_3][R_1\text{-}NH_2]}{(k_{-1}+k_2)} \quad (7)$$

Substituting Eq. 7 into Eq. 5 yields

$$\frac{-d[R_1\text{-}NH_2]}{dt} = \left(\frac{k_1k_2}{k_{-1}+k_2}\right)[R_2\text{-CO-}R_3][R_1\text{-}NH_2] \quad (8)$$

If one assumes $k_2 \ggg k_{-1}$,[39] then,

† Although the ^{13}C NMR data for compound **4** given in this reference were obtained in pyridine-d_5 and ours in D_2O at the same temperature, differences amounted to less than ±3 ppm in all the instances.

$$\frac{-\mathrm{d}[\mathrm{R_1\text{-}NH_2}]}{\mathrm{d}t} = k_1[\mathrm{R_2\text{-}CO\text{-}R_3}][\mathrm{R_1\text{-}NH_2}] \quad (9)$$

Acetol in solution occurs as two different tautomers with the carbonyl group in free (R_2-CO-R_3) and hydrated form (R_2-C(OH)$_2$-R_3). The dehydration equilibrium constant is given by

$$K_4 = \frac{[\mathrm{R_2\text{-}CO\text{-}R_3}]}{[\mathrm{R_2\text{-}C(OH)_2\text{-}R_3}]} \quad (10)$$

On the other hand, the Amadori compounds **3** and **4** also exhibit cyclic forms of the type shown in Scheme 1 (R_2-C(OH)(OR′)-R_3). The corresponding tautomer equilibrium constant is[‡]

$$K_5 = \frac{[\mathrm{R_2\text{-}CO\text{-}R_3}]}{[\mathrm{R_2\text{-}C(OH)(OR')\text{-}R_3}]} \quad (11)$$

Based on the applicable mass balance,

$$[\mathrm{R_2\text{-}CO\text{-}R_3}]_T = [\mathrm{R_2\text{-}CO\text{-}R_3}] + [\mathrm{R_2\text{-}C(OH)(OR')\text{-}R_3}] \quad (12)$$

it follows that

$$[\mathrm{R_2\text{-}CO\text{-}R_3}] = \frac{K_5[\mathrm{R_2\text{-}CO\text{-}R_3}]_T}{1+K_5} \quad (13)$$

Under the experimental conditions used, pyridoxamine occurs as a single ionic form with three tautomers in equilibrium of which only **1a** can react with Amadori compounds. Therefore, we must consider the tautomeric equilibrium between the aminomethyl and phenolate groups[46] as shown in Scheme 3. Based on it,

$$K_3 = \frac{[1a]}{[1b]+[1c]} \quad (14)$$

Also, based on the applicable mass balance,

$$[\mathrm{R_1\text{-}NH_2}]_T = [1a] + [1b] + [1c] \quad (15)$$

it follows that

$$[1a] = \frac{K_3[\mathrm{R_1\text{-}NH_2}]_T}{1+K_3} \quad (16)$$

Substitution of Eqs. 13 and 16 into Eq. 9 yields

$$\frac{-\mathrm{d}[1a]}{dt} = \frac{-\mathrm{d}[\mathrm{R_1\text{-}NH_2}]_T}{\mathrm{d}t} = k_1\frac{K_3K_5[\mathrm{R_2\text{-}CO\text{-}R_3}]_T[\mathrm{R_1\text{-}NH_2}]_T}{1+K_3+K_5+K_3K_5} \quad (17)$$

where

$$k_{\mathrm{obs}} = \frac{k_1K_3K_5[\mathrm{R_2\text{-}CO\text{-}R_3}]_T}{1+K_3+K_5+K_3K_5} \quad (18)$$

Therefore, Eq. 17 can be rewritten follows:

$$\frac{-\mathrm{d}[\mathrm{R_1-NH_2}]_T}{\mathrm{d}t} = k_{\mathrm{obs}}[\mathrm{R_1\text{-}NH_2}]_T \quad (19)$$

which can be integrated to

$$\ln\frac{[\mathrm{R_1\text{-}NH_2}]_T}{[\mathrm{R_1\text{-}NH_2}]_{T_0}} = -k_{\mathrm{obs}}t \quad (20)$$

At this point, k_{obs} can be calculated by fitting experimental data to Eq. 20.

When the nucleophile involved is the α-amino group in **5**, we only consider the second ionization equilibrium for such a group, due its low pK_a value that led us to despite the methylamine unprotonated tautomer specie corresponding to its monoprotonated ionic form

$$\mathrm{R_1\text{-}NH_3^+ + H_2O \rightleftharpoons R_1\text{-}NH_2 + H_3O^+} \quad (21)$$

the equilibrium constant for which is

$$K_6 = \frac{[\mathrm{R_1\text{-}NH_2}][\mathrm{H_3O^+}]}{[\mathrm{R_1\text{-}NH_3^+}]} \quad (22)$$

Taking into account that

$$[\mathrm{R_1\text{-}NH_2}]_T = [\mathrm{R_1\text{-}NH_2}] + [\mathrm{R_1\text{-}NH_3^+}] \quad (23)$$

Eq. 22 can be rewritten as

$$[\mathrm{R_1\text{-}NH_2}] = \frac{K_6[\mathrm{R_1\text{-}NH_2}]_T}{[\mathrm{H_3O^+}]+K_6} \quad (24)$$

Therefore, a reasoning similar to that used for compound **1** leads to Eq. 18, where k_{obs} is now given by

$$k_{\mathrm{obs}} = \frac{k_1K_6K_5[\mathrm{R_2\text{-}CO\text{-}R_3}]_T}{[H^+]+K_6+[H^+]K_5+K_6K_5} \quad (25)$$

4.10. Theoretical methodology

In order to justify the differences between the k_1 values for the reactions of **1** and **5**, the structure **1a** and the unprotonated form of **5** were optimized semi-empirically by using PM3 Hamiltonian[47] included in the software AMPAC v.8.0 (AMPAC 8, © 1992-2004 Semichem, Inc., PO Box 1649, Shawnee, KS 66222). The solvent effect was included in the calculations by using the COSMO continuum method[48] as implemented in AMPAC. Charges on the nitrogen atom in the α-amino group of **1** and **5** were calculated by using Mulliken[49] and Kollman[50] methods.

Acknowledgments

This work was made possible by a grant from the Spanish Government (DGICYT CTQ 2005-00250) and from the Balearic Government (PROGECIB-28A).

Supplementary data

Supplementary data associated with this article can be found, in the online version, at doi:10.1016/j.bmc.2008.04.002.

References and notes

1. (a) Ledl, F.; Schleicher, E. *Angew. Chem. Int. Ed. Engl.* **1990**, *29*, 565; (b) Thorpe, S. R.; Baynes, J. W. *Drugs*

[‡]The mathematical development that follows applies to the tautomeric equilibrium for compound **3** (or **4**), but can be extended to acetol by using K_4.

Aging **1996**, *9*, 69; (c) Friedman, E. A. *Diabetes care* **1999**, *22*, B65; (d) Baynes, J. W.; Thorpe, S. R. *Free Radical Biol. Med.* **2000**, *28*, 1708; (e) Ulrich, P.; Cerami, A. *Recent Prog. Horm. Res.* **2001**, *56*, 1.
2. (a) Horvat, S.; Jakas, A. *J. Pept. Sci.* **2004**, *10*, 119; (b) Takeuchi, M.; Yamagishi, S.; Iwaki, M.; Nakamura, K.; Imaizumi, T. *Int. J. Clin. Pharm. Res.* **2004**, *24*, 95; (c) Thorpe, S. R.; Baynes, J. W. *Amino acids* **2003**, *25*, 275; (d) Wautier, J-L. J.-L.; Schmidt, A. M. *Circ. Res.* **2004**, *95*, 233; (e) Monnier, V. M. *Arch. Biochem. Biophys.* **2003**, *419*, 1.
3. (a) Kume, S.; Takeya, M.; Mori, T.; Araki, N.; Suzuki, H.; Horiuchi, S.; Kodama, T.; Miyauchi, Y.; Takahashi, K. *Am. J. Pathol.* **1995**, *147*, 654; (b) Itakura, K.; Furuhata, A.; Shibata, N.; Kobayashi, M.; Uchida, K. *Biochem. Biophys. Res. Commun.* **2003**, *308*, 452; (c) Lee, W. K.; Bell, J.; Kilpatrick, E.; Hayes, M.; Lindop, G. B. M.; Dominiczak, M. H. *Artherosclerosis* **1993**, *98*, 219; (d) Rojas, A.; Morales, M. A. *Life Sci.* **2004**, *76*, 715.
4. (a) Miyata, T.; Van Ypersele De Strihou, C.; Kurokawa, K.; Baynes, J. W. *Kidney Int.* **1999**, *55*, 389; (b) Bohlender, J. M.; Franke, S.; Stein, G.; Wolf, G. *Am. J. Physiol. Renal Physiol.* **2005**, *289*, 645; (c) Mitsuhashi, T.; Nakayama, H.; Itoh, T.; Kuwajima, S.; Aoki, S.; Atsumi, T.; Koike, T. *Diabetes* **1993**, *42*, 826; (d) Waanders, F.; Greven, W. L.; Baynes, J. W.; Thorpe, S. R.; Kramer, A. B.; Nagai, R.; Sakata, N.; van Goor, H.; Navis, G. *Nephrol. Dial. Transpl.* **2005**, *20*, 2060.
5. (a) Reddy, V. P.; Obrenovich, M. E.; Atwood, C. S.; Perry, G.; Smith, M. *Neurotox. Res.* **2002**, *4*, 191; (b) Hoyer, S. J. *J. Neural. Transm.* **2002**, *109*, 341; (c) Choei, H.; Sasakui, N.; Takeuchi, M.; Yoshida, T.; Ukai, W.; Yamagishi, S.; Kikuchi, S.; Saito, T. *Acta Neurophatol.* **2004**, *108*, 189; (d) Colaco, C. A. L. S.; Harrington, C. R. *CNS Drugs* **1996**, *6*, 167.
6. (a) Crabbe, M. J. *Cell. Mol. Biol.* **1998**, *44*, 1047; (b) Stitt, A. W. *Ann. NY. Acad. Sci.* **2005**, *1043*, 582; (c) Shamsi, F. A.; Sharkey, E.; Creighton, D.; Nagaraj, R. H. *Exp. Eye Res.* **2000**, *70*, 369; (d) Biemel, K. M.; Friedl, D. A.; Lederer, M. O. *J. Biol. Chem.* **2002**, *277*, 24907.
7. Münch, G.; Schicktanz, D.; Behme, A.; Gerlach, M.; Riederer, P.; Palm, D.; Schinzel, R. *Nat. Biotechnol.* **1999**, *17*, 1006.
8. (a) Yaylayan, V. A.; Huyghues-Despointes, A. *Crit. Rev. Food Sci.* **1994**, *34*, 321; (b) Hodge, J. E. *Adv. Carbohydr. Chem.* **1955**, *10*, 169; (c) Hodge, J. E.; Rist, C. E. *J. Am. Chem. Soc.* **1953**, *75*, 316.
9. Thornalley, P.; Wolff, S.; Crabbe, J.; Stern, A. *Biochim. Biophys. Acta* **1984**, *797*, 276.
10. Smith, P.; Thornalley, P. *Eur. J. Biochem.* **1992**, *210*, 729.
11. Estendorfer, S.; Ledl, F.; Severin, T. *Angew. Chem. Int. Ed. Engl.* **1990**, *29*, 536.
12. Vasan, S.; Zhang, X.; Zhang, X.; Kapurniotu, A.; Bernhagen, J.; Teichberg, S.; Basgen, J.; Wagle, D.; Shih, D.; Terlecky, I.; Bucala, R.; Cerami, A.; Egan, J.; Ulrich, P. *Nature* **1996**, *382*, 275.
13. (a) Akira, K.; Hashimoto, T. *Biol. Pharm. Bull.* **2005**, *28*, 344; (b) Davidek, T.; Blank, I. *Chimia* **2005**, *59*, 862; (c) Wolf, G. *Eur. J. Clin. Invest.* **2004**, *34*, 785.
14. Yue, K. D.; McLennan, S.; Turtle, J. R. *Diabetologia* **1983**, *24*, 377.
15. Peyroux, J.; Sternberg, M. *Pathol. Biol.* **2006**, *54*, 405.
16. (a) Voziyan, P. A.; Hudson, B. G. *Ann. NY Acad. Sci.* **2005**, *1043*, 807; (b) Voziyan, P. A.; Khalifah, R. G.; Thibaudeau, C.; Yildiz, A.; Jacob, J.; Serianni, A. S.; Hudson, B. G. *J. Biol. Chem.* **2003**, *278*, 46616; (c) Voziyan, P. A.; Metz, T. O.; Baynes, J. W.; Hudson, B. G. *J. Biol. Chem.* **2002**, *277*, 3397; (d) Booth, A. A.; Khalifah, R. G.; Tood, P.; Hudson, B. G. *J. Biol. Chem.* **1997**, *272*, 5430; (e) Booth, A. A.; Khalifah, R. G.; Hudson, B. G. *Biochem. Biophys. Res. Commun.* **1996**, *220*, 113; (f) Khalifah, R. G.; Baynes, J. W.; Hudson, B. G. *Biochem. Biophys. Res. Commun.* **1999**, *257*, 251; (g) Price, D. L.; Rhett, P. M.; Thorpe, S. R.; Baynes, J. W. *J. Biol. Chem.* **2001**, *276*, 48967.
17. (a) Adrover, M.; Vilanova, B.; Muñoz, F.; Donoso, J. *Chem. Biodivers.* **2005**, *2*, 964; (b) Adrover, M.; Vilanova, B.; Muñoz, F.; Donoso, J. *Int. J. Chem. Kinet.* **2007**, *39*, 154.
18. Davies, S. S.; Brantley, E. J.; Voziyan, P. A.; Amarnath, V.; Zagol-Ikapitte, I.; Boutaud, O.; Hudson, B. G.; Oates, J. A.; Roberts, L. J. *Biochemistry* **2006**, *45*, 15756.
19. Zyzak, D.; Richardson, J. M.; Thorpe, S. R.; Baynes, J. W. *Arch. Biochem. Biophys.* **1995**, *316*, 547.
20. Reichard, G. A.; Skutches, C. L.; Hoeldtke, R. D.; Owen, O. E. *Diabetes* **1986**, *35*, 668.
21. Kalapos, M. P. *Med. Hypotheses* **1999**, *53*, 236.
22. Crugeiras, J.; Rios, A.; Amyes, T. L.; Richard, J. P. *Org. Biomol. Chem.* **2005**, *3*, 2145.
23. Love, P.; Cohen, R. B.; Taft, R. W. *J. Am. Chem. Soc.* **1968**, *90*, 2455.
24. Glushonok, G. K.; Glushonok, T. G.; Maslovskaya, L. A.; Shadyro, O. I. *Russ. J. Gen. Chem.* **2003**, *73*, 1027.
25. Yaylayan, V.; Forage, N. G. *J. Agric. Food Chem.* **1991**, *39*, 361.
26. Franklin, K. J.; Richardson, M. F. *Inorg. Chem.* **1980**, *19*, 2107.
27. Thompson, D. M.; Balenovich, W.; Hornich, L. H. M.; Richardson, M. F. *Inorg. Chim. Acta* **1980**, *46*, 199.
28. Irving, H.; Williams, R. J. P. *J. Chem. Soc.* **1953**, 3192.
29. Degenhardt, T. P.; Alderson, N. L.; Arrington, D. D.; Beattie, R. J.; Basgen, J. M.; Steffes, M. W.; Thorpe, S. R.; Baynes, J. W. *Kidney Int.* **2002**, *61*, 939.
30. Seiler, H. G.; Sigel, A.; Sigel, H. In *Handbook on metals Metalsin clinical Clinicaland analytical chemistryAnalytical Chemistry*; Seiler, H., Ed.; Marcel Dekker, Inc.: New York, 1987; p 40, Chapter 3.
31. Aitken, D. J.; Albinati, A.; Gautier, A.; Husson, H-P.; Morgant, G.; Nguyen-Huy, D.; Kozelka, J.; Lemoine, P.; Ongeri, S.; Rizzato, S.; Viossat, B. *Eur. J. Inorg. Chem.* **2007**, 3327.
32. Cussimanio, B. L.; Booth, A. A.; Todd, P.; Hudson, B. G.; Khalifah, R. G. *Biophys. Chem.* **2003**, *105*, 743.
33. Doddrell, D. M.; Pegg, D. T.; Bendall, M. R. *J. Magn. Reson.* **1982**, *48*, 323.
34. Derone, A. E. In *Modern NMR Techniques for Chemistry Research*; Baldwin, J. E., Ed.; Pergamon Press: New York, 1987, Chapter 9.
35. Beksan, E.; Schieberle, P.; Robert, F.; Blank, I.; Fay, L. B.; Schlichtherle-Cerny, H.; Hofmann, T. *J. Agric. Food Chem.* **2003**, *51*, 5428.
36. Röper, H.; Röper, S.; Heyns, K. *Carbohydr. Res.* **1983**, *116*, 183.
37. SigmaPlot. SigmaPlot Version 9.0. SPSS, Chicago, Illinois, USA, 2005.
38. (a) Borch, R. F.; Bernstein, M. D.; Durst, H. D. *J. Am. Chem. Soc.* **1971**, *93*, 2897; (b) Jentoft, N.; Dearborn, D. G. *J. Biol. Chem.* **1979**, *254*, 4359.
39. Bunn, H. F.; Higgins, P. J. *Science* **1981**, *213*, 222.
40. Gidley, M. C.; Sanders, J. K. M. *Biochem. J.* **1982**, *203*, 331.
41. Tonkovic, M.; Jakas, A.; Horvat, S. *BioMetals* **1996**, *9*, 55.
42. Cappannelli, M.; Gaggelli, E.; Jezowska-Bojczuk, M.; Molteni, E.; Mucha, A.; Porciatti, E.; Valensin, D.; Valensin, G. *J. Inorg. Biochem.* **2007**, *101*, 1005.
43. Kleszczewska, E. *Pol. J. Environ. Stud.* **1999**, *8*, 313.

44. Tonkovic, M.; Hadzija, O.; Ladesic, B.; Klaic, B.; Music, S. *Inorg. Chim. Acta* **1989**, *161*, 81.
45. Funke, W.; Klemer, A. *Carbohydr. Res.* **1976**, *50*, 9.
46. Metzler, D. E.; Harris, C. M.; Johnson, R. J.; Siano, D. B.; Thomson, J. A. *Biochemistry* **1973**, *12*, 5377.
47. Stewart, J. J. P. *J. Comput. Chem.* **1989**, *10*, 209.
48. Klamt, A. *J. Phys. Chem.* **1995**, *99*, 2224.
49. Mulliken, R. S. *J. Chem. Phys.* **1955**, *23*, 1833.
50. Besler, B. H.; Mertz, K. M.; Kollman, P. A. *J. Comput. Chem.* **1990**, *11*, 431.